LRU - LIGHTWEIGHT ROVER UNIT

A. Wedler[(1)], B. Rebele[(1)], J. Reill[(1)], M. Suppa[(1)], H. Hirschmüller[(1)], C. Brand[(1)], M. Schuster[(1)], B. Vodermayer[(1)], H. Gmeiner[(1)], A. Maier[(1)], B. Willberg[(1)], K. Bussmann[(1)], F. Wappler[(1)], M. Hellerer[(2)], R. Lichtenheldt[(2)]

[(1)] DLR - German Aerospace Center, Institute of Robotics and Mechatronics (Germany), armin.wedler@dlr.de
[(2)] DLR - German Aerospace Center, Institute of System Dynamics and Control (Germany), matthias.hellerer@dlr.de

ABSTRACT

This paper presents the novel Lightweight Rover Unit (LRU) developed at DLR-RMC Robotic and Mechatronic Center. The LRU rover is a terrestrial prototype based on the experiences gained with the mobile payload element (MPE) rover which has been originally developed for the ESA lunar lander mission. The small MPE lunar rover was foreseen for collecting and fetching samples on the lunar surface. This paper describes the development of the small and lightweight LRU rover prototype with respect to kinematic aspects, the electronic perspective and the control point of view. The LRU is equipped with a highly sophisticated autonomous navigation system, which is also briefly described in this paper. The LRU paves the way towards a small space qualified exploration rover. The technology readiness level (TRL) of its incorporated substantial robotic modules has been increased and the components and technologies developed for the LRU can be reused for future developments.

1. INTRODUCTION

The Lightweight Rover Unit LRU from DLR–RMC is a new innovative mobility device tailored to the needs of planetary exploration and terrestrial search and rescue applications. It is designed to operate and to manipulate objects on moderate to challenging terrain e.g. for fetching and handling samples and it allows exploration of large areas in a fast and efficient manner.

Due to its lightweight design and total mass of less than 30 kg, it is a promising additional payload for any future lunar mission. The rover concept is strongly inspired by the Lunar Lander Mobile Payload Element (MPE) and is in line with similar intended international planetary exploration missions e.g. ongoing Russian or Indian plans for small lunar mobility vehicles.

The design of the rover system is based on DLR's long experience in designing lightweight actuator units and robotic systems. The overall design process is continuously supported by simulation and a detailed evaluation of the performance even before hardware is available. The concurrent engineering workflow allows efficient and reliable design. The LRU rover locomotion subsystem (LSS) and its potential suitability for space applications have been given highest priority. The LSS has therefore been designed in a space qualifiable manner and a future upgrade to a fully space qualified version has been considered from the very beginning respectively. The four wheeled LSS system is fully steerable. All LSS actuator units are based on a combination of a powerful brushless DC motor and a harmonic drive gear box. In addition to the four wheel actuators and four steering actuators two serial elastic bogie actuators allow to actively control the front and rear bogie joints. This allows e.g. controlling the load distribution to the wheels and the body orientation while maintaining the advantages of passive suspension. The wheels design, also a combination of rigid (e.g. tire tread) and flexible (spokes) elements, is additionally supporting fast and efficient driving in rough terrain. The lightweight design, the advanced kinematics and the unique combination of active and passive chassis elements result in a very high traffic ability, terrainability and overall mobility performance.

Figure 1: The LRU in rough terrain.

The rover body and related remaining subsystems like power electronics, battery and communication are designed for terrestrial applications and based on reliable and cost-efficient commercially available components-off-the-shelf (COTS) as development time and performance have been the main design drivers. Finally a commercially available complete robotic arm is integrated to enable mobile manipulation with the rover. In order to fully exploit the capacity of the mobile system, an appropriate navigation algorithm and autonomy is implemented. Such high level control algorithms, e.g. the implemented autonomous way point navigation, are key elements for future exploration missions. As they strongly rely on perception sensors like cameras, the rover system includes a novel PanTilt

Unit incorporating a stereo camera. The PanTilt Unit has been designed and optimized for the requirements of this mobile system operation in rough terrain.
Within this paper the complete mechatronic development along with the structure of the entire mobile system are described and the development process is shown. Furthermore the high level control and autonomy system as well as the low level control system are explained. Finally the overall system has been tested in our planetary testbeds and labs. Results and experiences gained so far are presented.
In early 2011 the German Space Agency DLR commissioned Kayser-Threde (now renamed to OHB) with the feasibility study of a Mobile Payload Element (MPE) and Kayser-Threde has assembled relevant German competences in space robotics and lunar science for this study. The Mobile Payload Element is designed to be a small, autonomous and innovative rover of ~14 kg for exploration of the environment and sampling in the vicinity of the envisaged landing site. Although the ESA Lunar Lander served as reference scenario for the MPE development, it is compatible to any alternative landing mission with a similar mission profile. MPE's novel capability will be the possibility to acquire and to precisely document samples from controlled surface as well as subsurface locations, to determine their geological context and to bring them back to its lander for analyses with the on-board instruments. Further the MPE is able to collect samples from shaded areas, which may increases the chances of detecting any lunar volatiles. With an operating range of more than 100 m, it will provide access to a vast area of scientificly interesting objects and locations. The present MPE payload includes cameras, a close-up imager and a mole as a sampling device. The LRU is a DLR-RMC prototype to further analyse the MPE concept and corresponding mission aims for small sample retrieval vehicles for lunar surface operations.

2. KINEMATIC STRUCTURE

The kinematic design of the LRU has been focused on high terrain capabilities. The locomotion sub system (LSS) of the LRU consists of four actuated wheels attached to two bogies.

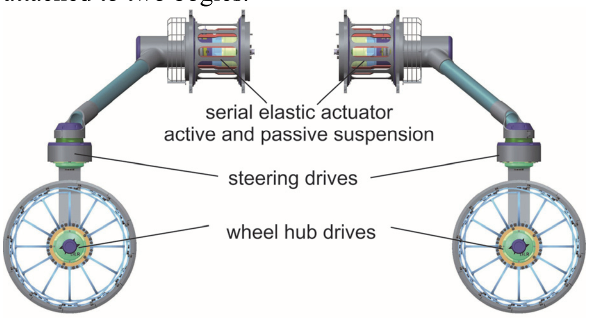

Figure 2: LRU LSS actuator distribution side view

One serial elastic actuator (SEA) unit per bogie guides the front and rear bogie independently. The two SEAs as well as the four wheel hub drives and the four steering drives are actuated by an ILM38 space drive train (see Chapter 3). The positions of these 10 LSS actuators are depicted in Figure 2.The LRU is designed to drive at a relatively high velocity of 1.11 m/s in rough terrain and dynamic loads resulting from undulating terrain and obstacles have to be considered. Therefore flexible wheel spokes (see Figure 6) and a passive suspension have been implemented which allow e.g. minimizing the shock loads and improving ground contact. The rotational spring of the SEA strongly contributes to the passive suspension of the LRU. It allows a passive rotation of up to 30° and includes a fluid damper in parallel.

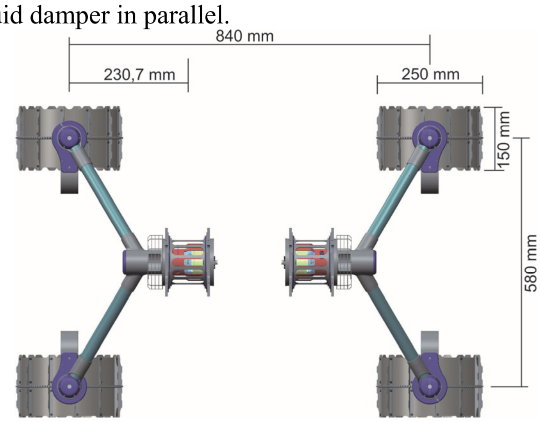

Figure 3: LRU LSS kinematic top view

Above that, the active element within the SEA, the actuator unit, allows controlling the bogie rotational positions and the resulting rover body position (see Figure 1). This allows adjusting the center of mass to improve its stability or to adjust the wheel load distribution. Active control of the wheel loads allows minimizing slip, improving ground contact or supporting obstacle negotiating. Furthermore, dynamic body damping can be achieved by actively controlling these actuators. As the camera beam is attached to the rover body, the body motion can also be used to reposition the camera head to get a better view of the environment or to avoid occultation by obstacles from different camera perspectives.

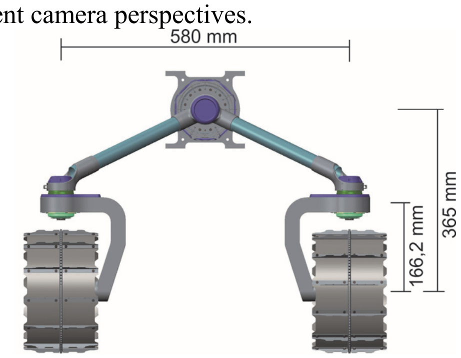

Figure 4: LRU LSS kinematic front view.

The LRU has a total length of 1090 mm and a total width of 730 mm. Figure 3 and Figure 4 show the main dimensions of the LSS of the LRU and depict the wheel and steering axis positions, the bogie joint position and the wheel dimensions. Even though not required for space applications, it shall be mentioned, that these overall dimensions facilitate handling significantly as they enable the LRU to drive through standard doors or fitting on a Euro-pallet.

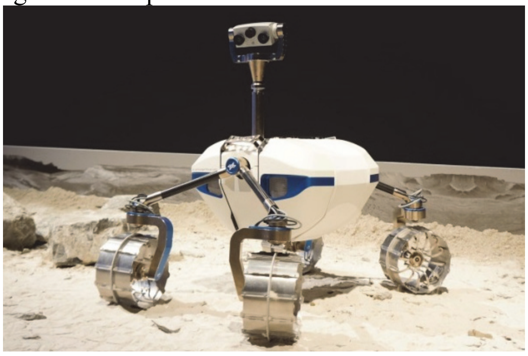

Figure 5: LRU Rover in sandy testbed.

Special attention has been paid to the wheel design and its dimensioning. The large wheel diameter and width in combination with flexible spokes lead to very good traction and grip in rough and stony terrain as well as in sandy environments. The lightweight design allows to reducing the wheel's weight to approx. 800 g (depending on spoke configuration).

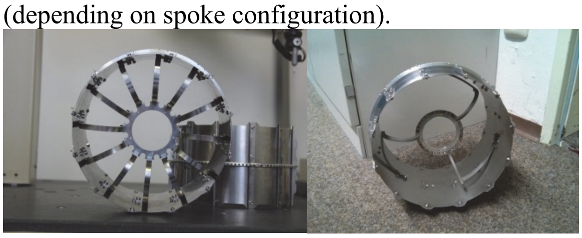

Figure 6: Two spoke configurations: Wheel equipped with 12 blade springs (left) and three laser sinter titan spokes (right).

The wheel design make use of the advantages of both, wide and narrow wheel types by combining a flexible spring metal sheet running surface with a central rigid ring. On hard flat terrain only the narrow rigid ring is in contact and a relatively low rolling resistance is achieved while on soft soil the large flexible running surface is engaged. The elastic wheel spokes form a suspension mechanism and allow absorbing shocks directly from the wheels. The wheel can be equipped with several configurations and types of spokes. Thereby the wheel stiffness can be adjusted. A maximum of 12 spokes can be used but also 6, 4, or simply 3 spokes per wheel are possible. Currently two spoke designs are available (see Figure 6). The first type of spokes makes use of simple bended blade springs. The second spoke design is characterized by a complex shape and has been FEM optimized for optimal force distribution while maintaining radial elasticity. The spokes have been manufactured by laser sintering and are made of homogenous titanium material.

The effective ground pressure (EGP) value has been introduced in [1] to allow a better comparison of different rover types and sizes and in [2] the simple model of EGP is presented. This simple model provides simple metric to compare a nominal ground pressure for vehicles with rigid wheels independent of the terrain.

Since the LRU weights approximately 30 kg, with a wheel diameter of 250 mm and a wheel width w of 150 mm the following ground pressure values can be calculated according to [2]:

$$EPG_{Earth} = \frac{F}{\mathrm{r} \cdot w} = \frac{73.5N}{0.25m \cdot 0.15m} = 1960\frac{N}{m^2} \quad (1)$$

$$EPG_{Lunar} = \frac{F}{\mathrm{r} \cdot w} = \frac{12.26N}{0.25m \cdot 0.15m} = 326.66\frac{N}{m^2} \quad (2)$$

3. MODULES AND SPACE QUALIFIABLE ELEMENTS

During the overall design process, the space application of different components and modules has been given highest priority and the related future space qualification process has been considered from the very beginning. Therefore the LRU development focuses on modules which will also be used in the MPE mission and are promising candidates for other national or ESA space projects, namely the drivetrains, the PanTilt mechanism and the autonomous payload element.

Since compact actuators are the key driver for both sub system designs, the LSS (locomotion sub system) and the PanTilt mechanism of the APE (Autonomous Payload Element) perception unit, these two actuator modules are described in the following.

The LRU actuators are based on the DLR-RMC Space Drive Unit series [3]. Currently two actuator sizes are available: The standard ILM38 Space Drive Unit (LSS) and a smaller ILM25 Space Drive Unit (PanTilt actuators). The motor name stands for internal-rotor motor with the number showing the diameter of the stator in millimetres. The experience and results gained so far with the ILM38 unit match partly with the smaller drive train versions and the design of the smaller unit strongly benefits from this knowledge. In general the units comprise the same design structure and are based on a Robodrive ® BLDC motor in combination with a single gear stage formed by a Harmonic Drive ® gear with a gear reduction ratio of 1:100. Two CAD models of the units are illustrated in Figure 7.

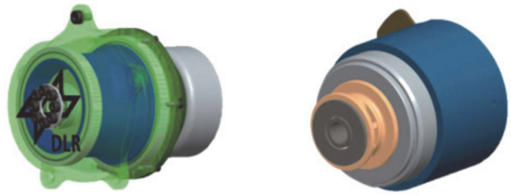

Figure 7: DLR-RMC RoboDrive Space Unit – left: ILM38 wheel hub unit – right: ILM25 DEXHAND Drive

Originally, the ILM38 wheel drive hub unit has been developed for the MPE rover prototype [4] and is therefore already well suited for planetary rovers. This means that the actuator unit already includes output bearing, contact flanges and a sealing system for a lunar regolith environment. The unit can be equipped with an output position sensor and is therefore also well suited for steering actuators. The detailed design of the ILM38 unit is depicted in Figure 8.

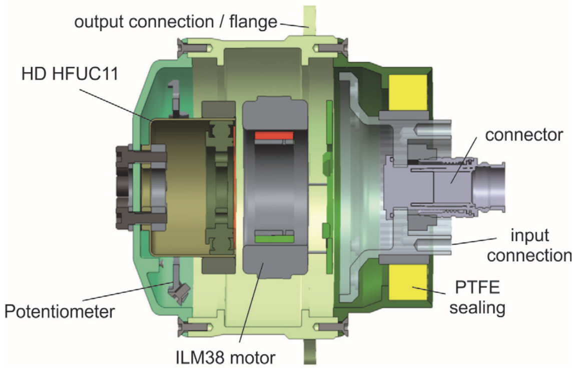

Figure 8: Section view of the ILM38 Space Drive Unit.

The cross section view in Figure 8 shows the ILM38 space unit with its essential elements. At the right side, the nominal input side is shown. This side of the units is fixed to the bogies and towards the rover body. The output flange provides a larger diameter and is part of the central housing element.

The Robodrive ILM38 motor (see *Table 1*) is combined with a single stage gear, a Harmonic Drive ® HFUC11. The unit itself includes a PTFE sealing system. The counterpart fixed to the input flange sub shall include an additional labyrinth sealing. Furthermore the figure shows the dense and compact integration of all components inside this light-weight unit. One main design guideline was a full enclosure of the unit. For EMC reasons a conductive enclosure has been implemented and a minimum material thickness of 1.5 mm aluminium is advantageous concerning radiation as well as w.r.t. thermal aspects.

The PanTilt Unit of the LRU rover is the most important perception instrument of the mobile system. The unit itself is depicted in Figure 9 and is described in detail in [5]. It is based on the ILM25 actuator modules and will be used for the LRU while aming as well on other space aiming mobility systems of DLR and its partners.

Figure 9: PanTilt Unit of the LRU rover

In contrast to the ILM38 unit, the ILM25 unit illustrated in Figure 10 is designed for operation in free space and has originally been developed for the two space projects DEXHAND [6, 7] and MASCOT [8, 9]. Therefore the unit does not include a final housing, enclosure, output guidance or sealing (see Figure 10) in its current version.

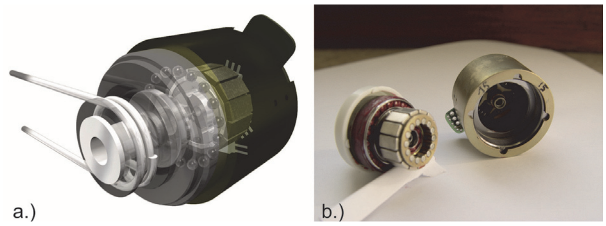

Figure 10: DLR-RMC RoboDrive 25 Space Unit: a) design rendering and b) the realized unit

As the ILM25 unit is currently applied within DEXHAND and MASCOT, it is undergoing a profound space qualification and testing program compared to the ILM38 unit. MASCOT is a DLR contribution to the Hayabusa-II mission that was launched in December 2014. The ILM25 has successfully accomplished a test run during health checks of the cruise phase. The data of motor and actuator of both units is summarized in *Table 1* and

Table *2*. Table 1 shows some details of the implemented plain Robodrive ® ILM motor itself, while Table 2 refers to an overview of the entire drive units values.

Table 1 ILM motor data

	ILM25	ILM38
Nominal motor power [W]	60	125
Nominal torque [Nm]	0.024	0.1
Peak torque [Nm]	0.10	0.35
Motor constant K_M [Nm/sqrt(W)]	0.012	0.039
Motor torque constant K_T [Nm/A]	0.008	0.021
Thermal resistance I	0.5	0.363

Table 2: Drive unit data

	ILM25	ILM38
Output flange [m]	approx. 0.05	0.07
Nominal output torque after gear [Nm]	2.4	5
Repeated peak torque [Nm]	4.6	11
Momentary peak torque [Nm]	9	25
Mass [kg]	approx. 0.2	0.36

4. ELECTRONICS AND COMPONENTS

The LRU incorporates a highly sophisticated energy management system that is monitored and controlled by the so called PSCDU i.e. the “power supply, control and distribution unit”. This subsystem’s fundamental requirements aim on a future usage in space. Thus, besides efficient energy management and durability, safety for the user, safety for the mission and safety for the equipment are in the limelight of the engineering efforts that are reflected by the comprehensive design.

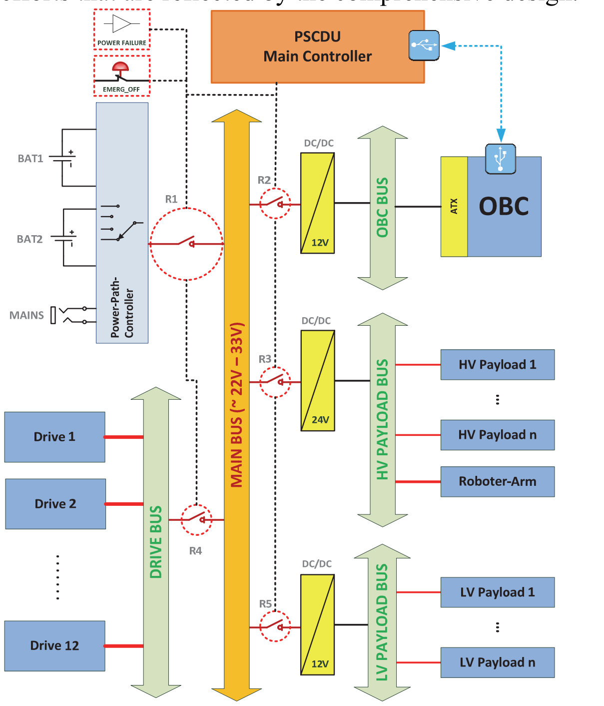

Figure 11: The PSCDU power backplane of the LRU

As shown in Figure 11, the PSCDU receives the incoming power from either rechargeable batteries (BAT1, BAT2) or an external power supply. The convenient power source is selected automatically according to its availability by an integrated power-path controller. The main PSCDU controller – along with further, distributed controllers for each bus segment – is responsible to switch power to the main bus and the system's sub busses and also to monitor voltage and currents on each bus segment. In case of a bus failure, the control system can disconnect the corresponding bus segment automatically. Moreover, as the PSCDU main controller is connected to the LRU on-board µITX Computer (OBC) via USB, commands can be sent to the PSCDU main controller from an external station to control the switching state of each bus segment. Also, the OBC can be provided with housekeeping messages about the status – i.e. voltage levels, current levels, switching states and failures – by the PSCDU main controller.

Originating from the power path controller, power is fed to the MAIN BUS without any conversion. The MAIN BUS then serves as central distribution-hub to the following sub busses:

- OBC BUS, contains a DC/DC converter with 12V output and powers the OBC and its subcomponents
- HIGH VOLTAGE PAYLOAD BUS, with DC/DC converter for 24V based payload, such as the robotic arm
- LOW VOLTAGE PAYLOAD BUS, with DC/DC converter for 12V based payload devices, such as external cameras and sensors
- DRIVE BUS, receives power directly from the MAIN BUS to supply the twelve drives of the LRU

Switching of the MAIN BUS and its subordinated bus segments is realized by bi-stable high current relays. The idea behind this relay configuration leads also to the safety requirements: in case of an electronics failure, the system's high level components, such as drives and OBC are able to proceed with their operation whereas the control station is aware of the occurred malfunction and can decide on further steps. To prevent high inrush currents when setting power, the PSCDU is equipped with a POWER FAILURE RESET unit that uses stored energy to assure that all relays are disconnected in case of a total power loss leading to a clean initial system state during the power-on phase. The current version of the PSCDU is prepared for future extensions by an incorporated extension interface.

5. AUTONOUMOUS DRIVING AND PERCEPTION SYSTEM

In the following we describe our perception and autonomy subsystems, analogue to the Autonomous Payload Element (APE) of the MPE project. The LRU Rover is equipped with a Xsens MTi-10 IMU for incremental inertial measurements and the PanTilt Unit including three cameras connected with a FireWire 800 hub. Two of them form a stereo camera system with a baseline of 9 cm. Stereo cameras are valuable RGBD sensors for outdoor and mixed indoor/outdoor environments. They are more lightweight than laser scanners, can cope with bright sunlight, in contrast to pattern projection based methods (e.g. Kinect), and provide high-resolution depth and additional greyscale/color data compared to Time of Flight (ToF) cameras. While the stereo pair is primarily used for navigation, the third camera can be adapted to the scientific requirements of a mission. We currently employ a color camera for object detection purposes. Our camera setup:

- Stereo cameras: f = 1.28 mm, Guppy PRO F-125B (1/3" chip size, resolution: 1292×964)
- Center camera: f = 1.28 mm, Guppy PRO F-125C (1/3" chip size, resolution: 1292×964)

All on-board computation is performed on an Intel Core i7-3740QM CPU (2.70 GHz) and an additional Spartan 6 LX75 FPGA for dense stereo matching (1024 × 508 at 14.6 Hz). We use a realtime kernel to ensure a deterministic operational response and hence low latency.

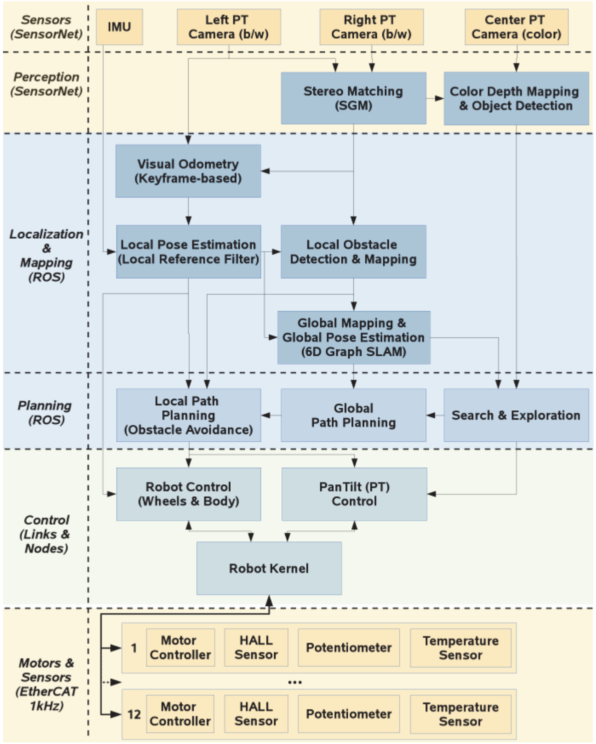

Figure 12: Software architecture block diagram

We present an overview of our software architecture in Figure 12. In the following, we introduce its key components and describe the data flow between them. In order to read the different perception sensors and for preprocessing, we use our SensorNet library. It is designed to provide a small and fast mechanism for distributing big data streams from different sensors, with low latency. Therefore, the software modules are segmented into different processes and the streaming data is provided via a shared memory interface from a server to a client application. We process the camera images by performing dense stereo matching using an FPGA implementation of the Semi-Global Matching (SGM) algorithm [10]. In addition, we map the image of the color camera onto the depth image for object detection. For high-frequency robust local pose estimation, we compute relative motion estimates from greyscale and depth data in our key-frame based visual odometry component [11] and fuse these with IMU measurements in an Extended Kalman Filter (EKF) with time-delay compensation [12]. We use the resulting estimates for fast local obstacle avoidance as well as to integrate the stereo-based depth data for local and global mapping. Our mapping pipeline consists of two parts. First we compute local obstacle maps of untraversable areas [13] that we employ for fast local path planning and obstacle avoidance. Second, we employ 6D graph SLAM methods to generate global 3D maps of the environment to be employed for global planning, search and exploration. We use the local obstacle maps to recognize places according to configurations of obstacles and thereby are able to generate loop closures in unstructured terrain. An example for a 3D map of our outdoor testbed is shown in Figure 13. We employ the Robot Operating System (ROS) as a middleware in order to connect the higher-level software components for localization, mapping and planning, which do not exhibit hard real-time requirements.

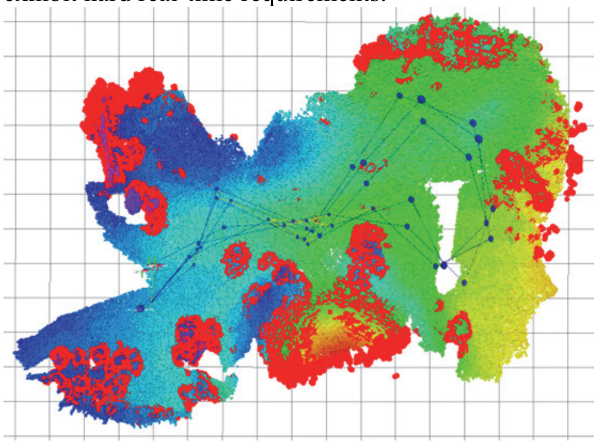

Figure 13: 3D Map of our outdoor testbed (height-colored) and obstacles (highlighted in red) generated by our mapping pipeline

In the control layer, see Figure 12, we use Links and Nodes, a middleware developed at DLR-RMC, to publish fixed size control-loop signals in realtime with low-latency using shared-memory and condition variables. In addition, Links and Nodes provides reliable, efficient and dynamically sized request-/response services via TCP remote procedure calls.

The Robot Kernel is a runtime-configurable robotic hardware abstraction framework. It is designed as a cross platform software component with reusable dynamically loadable device drivers encapsulated in modules. It provides an intra-module communication, a module synchronization mechanism and access to the hardware's cyclic and acyclic data. It also supplies modules with generic interfaces to control applications. For the communication between the Robot Kernel and the distributed motor controller units, we apply the realtime Master-Slave network EtherCat. Within a a reliably obtainable cycle time of 1ms we are able to transmit control and status packages throughout the serially connected components while achieving low jitter. The control loop runs with a frequency of 1 kHz, sending target control words to the motor controller units and returning the current motor states, as shown in Figure 14.

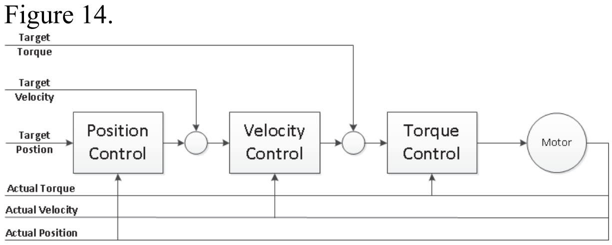

Figure 14: Motor controller

6. FIRST TEST RESULTS

Testing on component level allows cost effective testing at a very early stage of the project and before the entire system is available. For a first evaluation of the overall rover performance in general and in particular an analysis of the tractive performance of the LRU's actuator unit as well as the wheel, single wheel tests are performed using the conventional single wheel testbed (SWT) at DLR-RMC. The testbed features a parallel kinematics suspension as guidance in vertical direction and allows setting the velocity and wheel load. The translational motion towards the driving direction is not constrained, thus the resulting slip is dependent on the tractive forces. The tractive performance is rated by the measured slip, the tractive forces and torques. The soil used for the measurement campaign is the calcium carbide based DLR-RMCS-13.

Figure 15: Wheel track at v_t = 0.2 m/s

In loose condition it causes excessive sinkage and becomes almost impassable and can therefore be considered as a worst-case soft soil simulant for wheeled locomotion. However, by proper soil preparation and compaction, a wide variety of soil conditions can be achieved with this single soil simulant. Thus, it allows testing the wheel performance for a wide range of soil conditions without replacing the soil. The wheel and actuator performance has been tested for a carefully selected set of operational conditions (wheel load, wheel velocity and soil condition). For example, the torque-position dependency plot in Figure 16 shows the statistically processed data for a set of measurements at a single operational point.
In Figure 16 the wheel torque M_y is shown for nominal LRU-wheel load and a tangential velocity v_t of 0.2 m/s. For the relatively soft soil conditions and on levelled surface, a steady-state slip value of about 85% can be measured while still maintaining traversability and maneuverability of the rover. Figure 15 illustrates the respective qualitative behaviour of the wheel. Even though excessive wheel sinkage can be observed, the remaining wheel rut is almost entirely closed by the high rate of soil displaced to the rear.

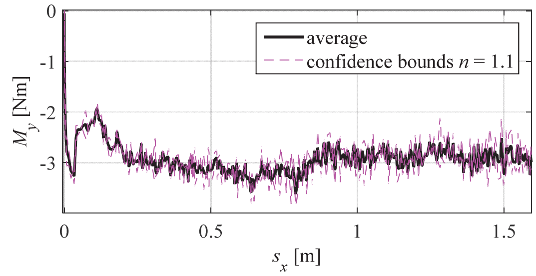

Figure 16 Wheel torque for v_t = 0.2 m/s

Additionally it can be observed, that the high sinkage and slip ratio does not coincide with high drive torques and due to the low wheel torque demand of only approx. 3 Nm, the energy consumption can be kept low.
In addition to the measurements at nominal wheel load, measurements with increased wheel loads were carried out in order to rate the tractive performance with increased payload mass. Summing up we found an applicable torque range of about 2.5 to 8.5 Nm for the LRU tractive gear at traversal of a soft simulant. The traction itself is mainly limited by the bearing capacity of the soil and excessive sinkage. It has also been observed that sinkage is speed dependent and tends to increase with wheel rotational velocity. Furthermore the measurement campaign will not only be used to rate the LRU's locomotion hardware, but also to further validate terra-mechanics models like SCM [14], novel approaches [15] and the particle-based framework DEMETRIA [16,17] for wheel-soil interaction, in order to improve future rovers' locomotion gear and control.

7. CONCLUSION

The LRU as the DLR-RMC's small planetary vehicle prototype has been presented regarding its kinematic structure, the space module based development process, the electronics infrastructure as well as its autonomous payload element. First performance results are comprised, in particular results from the wheel test on the single wheel test-bed have shown to be the key drivers for the wheel development. Especially the increase of knowledge about wheel elements, regarding traction and soil wheel interaction, is leading to further developments in hardware and validation of simulation software and numerical terramechanics models.
The autonomous navigation and assistance capabilities of the LRU system are key functionality's to enlarge the possibility of scientific use cases. This technology and corresponding hardware are research topics in the RMC aiming the further technological developments but also the space application and qualification.

In the near future the LRU will be used in the ROBEX lunar analogue demo mission [18] and the DLR SpaceBot Cup challenge in 2015. During the further use of the LRU system, but as well the accompanying module tests of the space developments, the goal of TRL increase will be in focus of investigations.

This work was supported by the Helmholtz Association, project alliance ROBEX, under contract number HA-304.

8. REFERENCES

1. Lindemann, R., (2011). Broader Interests and Applications, "The view of a JPL Hardware Engineer", Jet Propulsion Laboratory, California Institute of Technology

2. Heverly M., Matthews J, et al., (2013).Traverse Performance Characterization for the Mars Science Laboratory Rover., J. Field Robotics 30(6):835-846

3. Armin Wedler, Maxime Chalon et al., (2012). DLRs dynamic actuator modules for robotic space applications, 41st Aerospace Mechanisms Symposium, Vol 41

4. Haarmann, R., et al., (2012). Mobile Payload Element (MPE): Concept study for a sample fetching rover for the ESA Lunar Lander Mission, I-SAIRAS, Turin, Italy

5. Wedler, A., et al., (2013). Pan/Tilt unit as perception module for extra terrestrial vehicle and landing systems, Proc. of the 12th Symposium on Advanced Space Technologies in Robotics and Automation, Noordwijk, The Netherlands

6. Wedler, A., et al, (2011). DLRs space qualifiable multi-fingered DEXHAND, Proc. of the 11th Symposium on Advanced Space Technologies in Robotics and Automation (ASTRA), Noordwijk, The Netherlands.

7. Chalon, M. et al., (2015), Spacehand: a multi-fingered robotic hand for space ASTRA, Proc. of the 13th Symposium on Advanced Space Technologies in Robotics and Automation (ASTRA), Noordwijk, The Netherlands.

8. Reill J., et al., (2013). Development of a Mobility Drive Unit for Low Gravity Planetary Body Exploration, Proc. of the 12th Symposium on Advanced Space Technologies in Robotics and Automation, Noordwijk, The Netherlands

9. Reill J., Sedlmayr H.-J, et al., (2015). MASCOT – Asteroid Lander with Innovative Mobility Mechanism, Proc. of the 13th Symposium on Advanced Space Technologies in Robotics and Automation, Noordwijk, The Netherlands

10. Hirschmüller, H., (2008).Stereo Processing by Semi-Global Matching and Mutual Information, IEEE Transactions on Pattern Analysis and Machine Intelligence, vol. 30, no. 2, pp. 328–341

11. Hirschmüller H, Innocent, P., Garibaldi, J. (2002). Fast, Unconstrained Camera Motion Estimation from Stereo without Tracking and Robust Statistics, in International Conference on Control, Automation, Robotics and Vision

12. Schmid, K. , Ruess, F., et al., (2012). State Estimation for highly dynamic flying Systems using Key Frame Odometry with varying Time Delays, in IEEE/RSJ International Conference on Intelligent Robots and Systems

13. Brand, C., Schuster M., et al., (2014). Stereo-Vision Based Obstacle Mapping for Indoor/Outdoor SLAM, in IEEE/RSJ International Conference on Intelligent Robots and Systems.

14. Krenn R., Hirzinger G., (2009). SCM – A Soil Contact Model for multi-body system simulation, In 11th European Regional Conference of the International Society for Terrain-Vehicle Systems - ISTVS 2009, Bremen, Germany

15. Lichtenheldt R., et al., (2015). Heterogeneous, multi-tier wheel ground contact simulation for planetary exploration, ECCOMAS Thematic Conference on Multibody Dynamics, Barcelona, Spain

16. Lichtenheldt R., Schäfer B., (2013), Planetary Rover Locomotion on soft granular Soils - Efficient Adaption of the rolling Behaviour of nonspherical Grains for Discrete Element Simulations. In 3rd Int. Conference on Particle-Based Methods, S. 807-818, ISBN 978-84-941531-8-1, Stuttgart, Germany

17. Lichtenheldt R., et al., (2014). Hammering beneath the surface of Mars- Modeling and simulation of the impact-driven locomotion of the HP3-Mole by coupling enhanced multi-body dynamics and discrete element method, In 58th Ilmenau scientific colloquium (IWK), Ilmenau, Germany

18. Wedler, A., et al., (2015). ROBEX - Components and Methods for the Planetary Exploration Demonstration Mission, Proc. of the 13th Symposium on Advanced Space Technologies in Robotics and Automation , Noordwijk, The Netherlands.